ISBN: 978-3-95450-184-7 doi:10.18429/JACoW-IPAC2018-TUPMK009

ELECTRON BEAM OPTICS FOR THE ASU COMPACT XFEL*

C. Zhang†, W. S. Graves, M. R. Holl, L. E. Malin, ASU, Tempe, USA
E. A. Nanni, SLAC, Menlo Park, USA

Abstract

Arizona State University (ASU) is pursuing a new concept for a compact x-ray FEL (CXFEL) as a next phase of compact x-ray light source (CXLS). We describe the electron beam optics design for the ASU compact XFEL. In previous experiments we introduced a grating diffraction method to generate a spatially modulated beam. We plan to combine a telescope imaging system with emittance exchange (EEX) to magnify/demagnify the modulated beam and transfer it from transverse modulation into a longitudinal one to make it an ideal seed for a phase-coherent XFEL. The simulation results of the beam line setup will be demonstrated. Our first goal is to successfully image the modulated beam with desired magnification then we will investigate various magnification and magnets combinations and optimize aberration correction.

INTRODUCTION

As a next phase of ASU CXLS project, CXFEL design is developed from current beam optics and will be able to transform the incoherent ICS emission of CXLS into a fully coherent x-ray laser [1, 2] by using a recently developed method combining electron diffraction through patterned silicon crystal and EEX to create pre-nanobunched beam [3]. In previous experiments, we diffracted an electron beam with nanoscale grating on silicon crystal and obtained a periodical spacial modulated beam [4]. We here present new beam optics for CXFEL including a telescope system and bending dipoles which are designed to image the modulated beam at a desired distance.

The CXFEL layout is shown in Fig. 1 [5]. From the right end of the figure, a 4 MeV beam is generated by the 4.5 cell x-band photoinjector. The photoinjector is followed by three 35 cm long linac sections L1, L2, L3 which in total accelerate the beam to a maximum of 35 MeV. The diffraction silicon grating is located between linac section L1 and L2 and diffracts beam at a tunable energy with a maximum of 12 MeV. The optic design of the beam line has three main sections: nanopattern imaging section, EEX section and ICS interaction section. The imaging section follows linac setion L3 and is composed of 2 quadrupole triplets forming a telescope system. The EEX section consists of the 4 bend magnets B1-B4, an RF deflector cavity and accelerator cavity that are independently phased and powered, along with sextupoles S1-S3 and octopole O1 for aberration correction. After EEX, the interaction section starts with a focusing triplet that brings the beam size down to a micron at the ICS interaction point before colliding with ICS laser field. Downstream the IP point, two dipoles respectively bend the beam by 30 degrees horizontally and 90 degrees vertically into beam dump.

ASU CXLS is now under construction at MIT Bates Laboratory. As a direct upgrade of CXLS, CXFEL offers a effective way towards a smaller and less expensive XFEL while producing fully coherent x-ray output. Calculations and simulations in this paper are made based on current CXLS setup with the exception of the EEX line and will work as preliminary results to guide future construction of CXFEL.

TELESCOPE SYSTEM

We describe the simulation results of telescope system in imaging section. From previous diffraction experiment, the spatial modulated beam has a 400 nm period according to the groove width. In order to achieve a femtosecond 1 keV x-ray output performance for CXFEL design, a demagnification by a factor of hundred is required to bring the modulated beam to a few nanometer scale [3, 6]. We introduce two focal length coupled triplets as a telescope system which is capable to image beam at a magnification/demagnification about 10x.

The simulation setup of telescope section is shown in Fig. 2. In Fig. 2 (a), the modulated beam starts at x=0 m and the center of first triplet locates at 0.23 m downstream. From left to right, quadrupoles in first triplet each has a 0.01 m,0.02 m and 0.01 m length and 19.483 T/m, -18.69 T/m and 19.483 T/m field gradient. The spacing and field strength of first triplet was tuned to have a focal length f1 of 0.23 m that the modulated beam starts at the focal point of first triplet. For the second triplet centering at 2.49 m from start point, each of the quadrupoles has a 0.01 m,0.02 m and 0.01 m length and 6.2915 T/m, -6.2615 T/m and 6.2915 T/m field gradient.The spacing and field strength of second triplet was tuned to have a focal length f2 of 2.03 m. Noticing the spacing L between first and second triplet in this setup is 2.26 m which satisfy the telescope definition $L = f1 + f2$. A common equation used for telescope magnification as following

$$M = \frac{f_o}{f_e} \tag{1}$$

where f_o is the object focal length, f_e is the eyepiece focal length. In our case, $f_o = f1 = 0.23\ m$, $f_e = f2 = 2.03\ m$ gives a theoretical magnification $M = \frac{f_o}{f_e} = \frac{0.23}{2.03} = 0.113$ which is equivalent to have a demagnification of 8.82.

The simulation results in Fig. 2 (b)(c) matches up with the magnification calculation. In GPT setup, we started the beam

* Work supported by NSF awards 1632780, 1231306, DOE award DE-AC02-76SF00515 and ASU
† czhan178@asu.edu

ISBN: 978-3-95450-184-7 doi:10.18429/JACoW-IPAC2018-TUPMK009

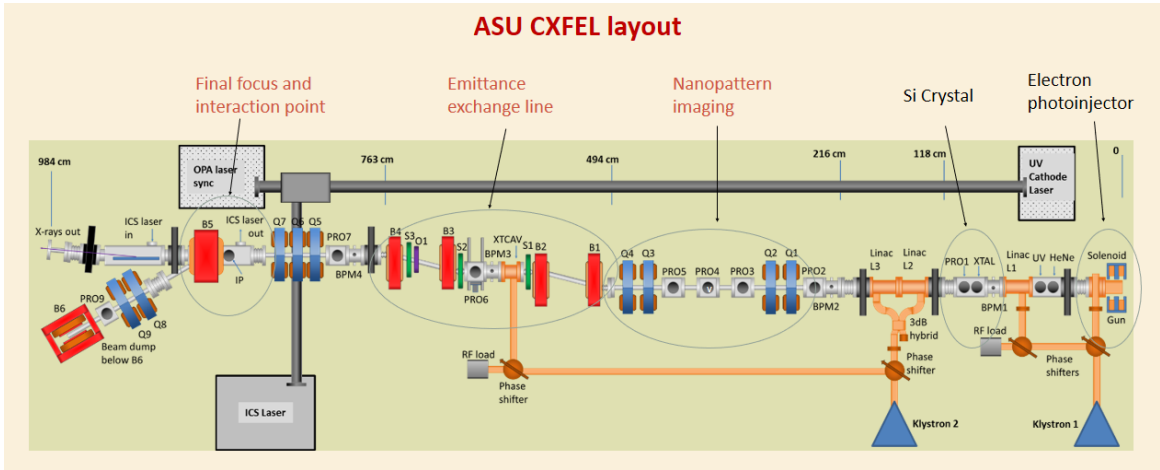

Figure 1: Major components of CXFEL. A telescope demagnifies the pattern and matches to the emittance exchange line before the laser interaction point. Then two dipoles bend the beam by 30 degrees horizontally and 90 degrees vertically into the beam dump.

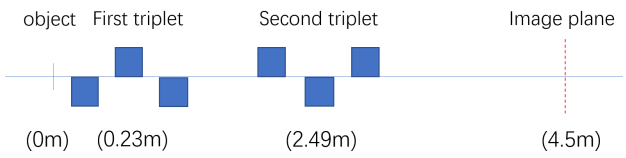

(a) Double triplets telescope setup and image plane

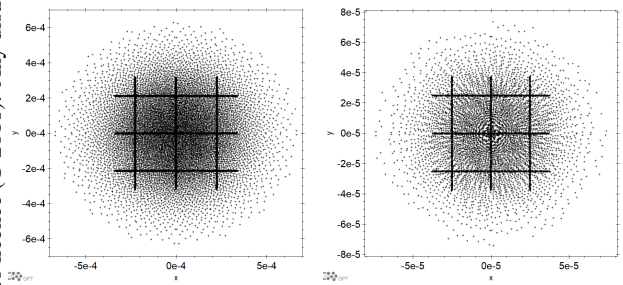

(b) Input beam (c) Snapshot at image plane

Figure 2: (a) Gives the telescope design and where the image plane locates. (b) and (c) shows General Particle Tracer (GPT) simulation results at start point and image plane.

at 4.4 MeV with a emittance of 10 nm and added several premade dense strips with a 220 microns spacing into the initial beam. The beam is then sent to telescope system and forms an image 4.5 m downstream. At image plane, the shape of crossing strips maintained a high symmetry compared with initial beam which means there is little astigmatism produced as beam traveling through this section. The final spacing between each strip at image plane is about 25 microns and gives a demagnification of entire section at $M = \frac{220}{25} = 8.8$ which very well matches up previous calculation.

To demagnify the initial modulated beam by a factor of hundred as previous discussed, we proposed to build up a two-stage telescope system that has two double triplet telescopes each of those has similar property as the one demonstrated above. First stage starts at the exit of the diffraction crystal and has a magnification M_1 while the second stage starts at the image plane of the first stage and has a magnification M_2. Thus a two-stage telescope system has a total magnification of $M_t = M_1 * M_2$ and image the demagnified beam to the image plane of second stage which would be the ideal ICS interaction point after EEX.

BENDING DIPOLE

From Fig. 1, the bending dipole B5 locates right after the ICS interaction point and deflect the beam by 30 degrees towards beam dump. Simulations of electrons bending angle versus traveling distance in dipole field were performed in order to guide the micron-size beam to hit right on ICS laser, Since the fringe field of the bending dipole extends towards interaction point.

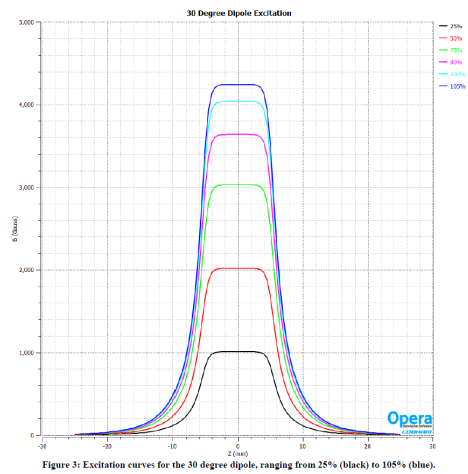

Figure 3: Excitation curves for the 30 degree dipole, ranging from 25% (black) to 105% (blue).

Figure 3: Excitation curves of 30 degrees bending dipole.

The excitation curves provided by the vendor Everson Tesla Incorporated are shown in Fig. 3. The bending dipole

ISBN: 978-3-95450-184-7 doi:10.18429/JACoW-IPAC2018-TUPMK009

has a iron core with a length of 100 mm and a gap of 27 mm. At 100% excitation, the nominal field of bending dipole is 0.404 T. The following Enge function Eq.(2) has been used to simulate the dipole field [7]

$$B_y(z, y = 0) = \frac{1}{1 + exp(b_1(z - dL))} \tag{2}$$

Where dL changes the effective length of the magnet, b_1 effects the steepness of the drop-off of the magnetic field.

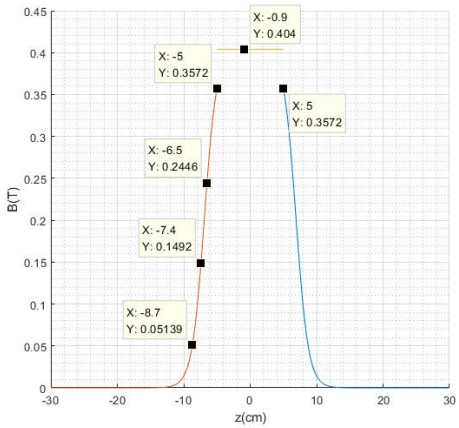

(a) Simulated dipole field

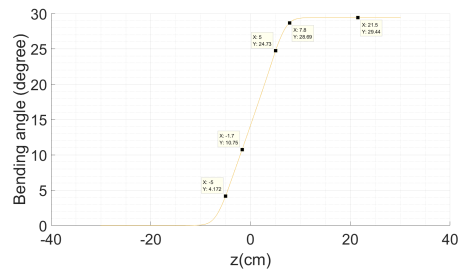

(b) Beam bending angle versus z as it traveling through bending dipole

Figure 4: Simulation results of 30 degrees bending dipole

The simulated dipole field is shown in fig. 4(a). The bending angle through simulated dipole field can be written as [8]

$$\theta = \int \frac{1}{\rho} dz = \frac{0.2998}{\beta E} \int |B| dz \tag{3}$$

The integral results are presented as a curve showing bending angle versus z in Fig. 4(b). The entire dipole field deflects the beam by 29.44 degrees with left and right fringe field bending about 4 degrees on each side. The ICS interaction point position needs a maximum 4 degrees compensation from the fringe field effect.

CONCLUSIONS

We have described current CXLS setup and optics design including telescope system and bending dipole for ASU CXFEL based on CXLS. The two-stage telescope design meets the transformation requirement to image the modulated beam downstream with a demagnification about 100x. The 30 degrees bending dipole field has been simulated along the beam trajectory. The bending angle versus z relation was generated to study the bending angle within fringed field area. Further work includes examine EEX setup and will focus on code test of the entire CXFEL design with all components correctly inserted.

ACKNOWLEDGEMENTS

We gratefully acknowledge support from NSF Division of Physics (Accelerator Science) award 1632780, the National Science Foundation BioXFEL Science and Technology Center funded by NSF award 1231306, and DOE grant DE-AC02-76SF00515.

REFERENCES

[1] W. S. Graves, F. X. Kärtner, D. E. Moncton, and P. Piot, "Intense superradiant x rays from a compact source using a nanocathode array and emittance exchange," *Phys. Rev. Lett.*, vol. 108, p. 263904, Jun 2012.

[2] W. S. Graves, J. Bessuille, P. Brown, S. Carbajo, V. Dolgashev, K.-H. Hong, E. Ihloff, B. Khaykovich, H. Lin, K. Murari, E. A. Nanni, G. Resta, S. Tantawi, L. E. Zapata, F. X. Kärtner, and D. E. Moncton, "Compact x-ray source based on burst-mode inverse compton scattering at 100 khz," *Phys. Rev. ST Accel. Beams*, vol. 17, p. 120701, Dec 2014.

[3] E. Nanni, W. Graves, and D. Moncton, "Nanomodulated electron beams via electron diffraction and emittance exchange for coherent x-ray generation," *Physical Review Accelerators and Beams*, vol. 21, 1 2018.

[4] L. Malin *et al.*, "Comparison of theory, simulation, and experiment for dynamical extinction of relativistic electron beams," in *Proc. of Int. Particle Accel. Conf (IPAC2017)*, (Copenhagen, Denmark), p. THPAB088, May 2017.

[5] W. Graves, J. Chen, P. Fromme, M. R. Holl, R. Kirian, L. Malin, K. Schmidt, J. Spence, M. Underhill, U. Weierstall, N. A. Zatsepin, C. Zhang, P. D. Brown, K. H. Hong, D. E. Moncton, E. A. Nanni, and C. Limborg-Deprey, "Arizona state university compact x-ray free electron laser," *Proc. of 2017 Int'l Free Electron Laser Conference (FEL2017)*, p. TUB03, August 2017.

[6] E. A. Nanni and W. S. Graves, "Aberration corrected emittance exchange," *Phys. Rev. ST Accel. Beams*, vol. 18, p. 084401, Aug 2015.

[7] B. D. Muratori, J. K. Jones, and A. Wolski, "Analytical expressions for fringe fields in multipole magnets," *Phys. Rev. ST Accel. Beams*, vol. 18, p. 064001, Jun 2015.

[8] H. Wiedemann, *Particle Accelerator Physics (Fourth Edition)*. New York: Springer, 2015.